

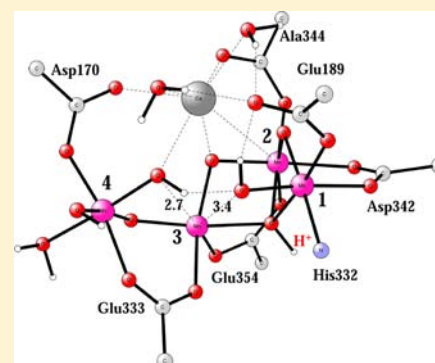
Substrate Water Exchange for the Oxygen Evolving Complex in PSII in the S_1 , S_2 , and S_3 States

Per E. M. Siegbahn*

Department of Organic Chemistry, Arrhenius Laboratory, Stockholm University, Stockholm SE-106 91, Sweden

S Supporting Information

ABSTRACT: Detailed mechanisms for substrate water exchange in the oxygen evolving complex in photosystem II have been determined with DFT methods for large models. Existing interpretations of the experimental water exchange results have been quite different. By many groups, these results have been the main argument against the water oxidation mechanism suggested by DFT, in which the oxygen molecule is formed between a bridging oxo and an oxyl radical ligand in the center of the OEC. That mechanism is otherwise in line with most experiments. The problem has been that the mechanism requires a rather fast exchange of a bridging oxo ligand, which is not a common finding for smaller Mn-containing model systems. However, other groups have actually favored a substrate derived oxo ligand partly based on the same experiments. In the present study, three S-states have been studied, and the rates have been well reproduced by the calculations. The surprising experimental finding that water exchange in S_1 is slower than the one in S_2 is reproduced and explained. The key to this rate difference is the ease by which one of the manganese centers (**Mn3**) is reduced. This reduction has to occur to release the substrate water from **Mn3**. The similar rate of the slow exchange in S_2 and S_3 has been rationalized on the basis of earlier experiments combined with the present calculations. The results strongly support the previous DFT-suggested water oxidation mechanism.



I. INTRODUCTION

The possibility to finally understand the mechanism of oxygen formation by the oxygen evolving complex (OEC) in photosystem II (PSII) has increased substantially during the past 5 years. There are two main reasons for this. First, X-ray structures of the enzymes are now available, initially at a low resolution of 2.9–3.5 Å,^{1–3} but recently at a high resolution of 1.9 Å.⁴ The second main reason is that the development of high accuracy quantum chemical cluster model calculations has improved to a stage where quantitative information can be obtained even for such a complicated system as PSII. The best example of this in the present context is that the structure predicted by model calculations some years ago⁵ is very similar to the new high-resolution X-ray structure. The constant increase of highly accurate information from spectroscopies, such as EXAFS,^{6–8} also significantly contributes to the present state of knowledge. However, even though the latter type of information is of high accuracy, it is very often difficult to make reliable and undisputable mechanistic interpretations from the spectroscopic data. The present study describes such an example, for substrate water exchange,^{9–13} where the interpretations have been quite different by different groups.^{14–16} This type of experiment is particularly important at the present stage, because it is the main experimental source of detailed mechanistic information for the actual O–O bond formation step. A review on water oxidation experiments for the OEC has recently been written.¹⁷

Studying substrate binding to the OEC experimentally is quite difficult, often requiring a combination of isotope labeling and time-resolved methods. The following techniques have been used: time-resolved isotope ratio membrane-inlet mass spectrometry, advanced EPR techniques such as ESEEM, ENDOR, and HYSCORE, ¹H NMR relaxation enhancement measurements, and FTIR difference spectroscopy.¹⁸ The most significant substrate water exchange results can be summarized as follows. In the S_0 -state, only one substrate water is observed to exchange at a rate of 10 s⁻¹. In S_1 , the substrate water exchanges at a rate of only 0.02 s⁻¹, and in S_2 the rate increases to 2 s⁻¹. In S_2 , a second substrate water is observed to exchange almost as fast as if it was not bound. In S_3 , there is a slow substrate water exchange at a rate of 2 s⁻¹, and a fast exchange at 40 s⁻¹. The two most interesting of these observations, both quite unexpected, are that the slow exchange is actually faster in S_2 than in S_1 , and that the slow exchange is the same in S_2 and S_3 .

A common interpretation of the general observations of the substrate oxygen exchange rates for manganese complexes (other than the OEC) can be summarized in the following way:¹⁵

- (1) Oxo groups in bridging positions between high valent Mn ions exchange extremely slowly (<10⁻² s⁻¹ for Mn₂(III,IV) and <10⁻⁶ s⁻¹ for Mn₂(IV,IV)).

Received: February 11, 2013

Published: June 6, 2013

- (2) Deprotonation of any water bound to a metal ion should increase the binding energy and thus decrease its exchange rate strongly.
- (3) Oxidation of Mn from III to IV should increase the binding strength of any water coordinated to that Mn, and thus decrease the exchange rate strongly (i.e., by several orders of magnitude).

When these general results were combined with measurements for the OEC, the following conclusions were drawn by Dau et al.:¹⁵

- (1) The increase in k_{slow} in the S_0 to S_1 transition might indicate water deprotonation.
- (2) For the increase of water exchange in the S_1 to S_2 transition, any simple model will fail. A hypothetical explanation related to a change of the pK value of a bridging oxide was suggested.
- (3) Substrate water molecules are not in bridging positions between Mn ions.
- (4) Deprotonation of any of the substrate waters is excluded in the S_2 to S_3 transition.
- (5) Substrate water molecules are not bound to the Mn ions that are oxidized in the S_2 to S_3 transition.

In summary, the following was suggested: In the three Mn-oxidizing S-state transitions (from S_2 to S_3), no substrate water is deprotonated, but rather two bases are created that can accept a proton from water in the process of O–O bond formation reaction. Even though most of these conclusions appear quite convincing, and are shared by many other groups, see, for example, refs 16,19, it is clear that they rely on a quite simplified picture, also admitted by the authors.

The above conclusions¹⁵ are in strong disagreement with cluster DFT studies indicating formation of the O–O bond between a terminal oxyl radical and a bridging oxo-group (a direct coupling (DC) mechanism).²⁰ Instead, they are more in line (but not quite) with an acid base (AB) mechanism, where the bond is formed after an attack by an outside water molecule, suggested in other DFT calculations.^{16,21} On the other hand, in several DFT studies, the AB mechanism has been excluded in comparisons to the DC mechanism, because the barrier was found to be very much higher.^{5,20} For the suggested AB mechanism to be consistent with the water exchange experiments for PSII, water has to be strongly bound to calcium. In fact, a very slow rate for exchange of water bound to calcium was obtained from a subsequent DFT study.¹⁶ However, this result is not consistent with the very fast water exchange observed for calcium complexes in solution of 10^8 s^{-1} .²²

A mechanism for O–O bond formation, much more in line with the theoretical DC mechanism, has been suggested by Messinger based on the same data as outlined above.^{14,23} The slowly exchanging water in S_3 has there been considered to be a bridging oxo group, while the fast one would be a terminal hydroxo ligand. Still, the proposal was claimed to be in line with the water exchange data. A major reason for the assignment of the position of the slowly exchanging water was that it is likely to be in a bridging position between two manganese and calcium in S_0 , because its deprotonation in the S_0 to S_1 transition shortens one Mn–Mn distance according to EXAFS.⁸ Arguments relating to Ca/Sr substitution, pH, and isotope effects were also used.^{10,17,23}

Very recently, while the present work was under way, there have been some other important experiments relating to water

exchange. A major experimental breakthrough was reached in a study by Rapatskiy et al.²⁴ They were able to suggest which oxygens in the S_2 -state that were most likely to form dioxygen, by a combination of ELDOR and water exchange experiments. The slowly exchanging oxygen was proposed to be one of the central oxo-groups in agreement with the DFT mechanism.^{20,25–27} The second substrate water was suggested to bind in connection with formation of the S_3 -state, as was also suggested by previous experiments,¹³ and by DFT calculations using independent arguments.⁵ These results were at variance with the conclusions of an earlier, but recent, experimental study of model systems and of manganese catalase by Connell et al.,¹⁹ where water exchange of an oxo group was found to be very much slower than the slow water exchange in the OEC, suggesting that an oxo group could not be a substrate in PSII.

In the present study, a few different cases of water exchange for the OEC will be treated by hybrid DFT methods. The cases include the slow water exchange in S_1 and S_2 , the slow and fast water exchange in S_3 , and water exchange of water bound to calcium. It will be shown that water exchange can involve very complicated processes with many steps that are difficult, or almost impossible, to predict without detailed calculations.

II. METHODS AND MODELS

The density functional theory (DFT) calculations discussed here were made using the hybrid functional B3LYP*, which is a modification of the original B3LYP functional²⁸ with a reduction of the exact exchange to 15%.²⁹ Procedures used were very similar to those in previous studies,^{5,25,27} with polarized basis sets for the geometries (lacvp*), large basis sets for energies (cc-pvtz(-f)), and a surrounding dielectric medium with dielectric constant equal to 6.0 (basis lacvp*). Dispersion effects were added using the empirical formula by Grimme.³⁰ The performance of the B3LYP functional for the present type of problems has been reviewed,³¹ indicating a typical accuracy within 3–5 kcal/mol, normally overestimating barriers. The calculations were performed with the programs Jaguar³² and Gaussian 09.³³

The transition states for the large model were obtained by first fully optimizing the TS for a smaller model with about 100 atoms with the lacvp basis set, and then keeping the most important distances frozen from the small model. The zero-point effects were obtained for a still smaller model of about 70 atoms but with the larger lacvp* basis set.

The quantum chemical cluster model chosen for the present applications is the same as the one used in the most recent studies.^{27,34} The model is based on the high-resolution (1.9 Å) structure by Shen et al.,⁴ and is seen for the S_2 -state in Figure 1, where only the most important atoms are shown. The full 200-atom structure is given as Supporting Information. The amino acids included in the model are first the directly binding amino acids, Asp170, Glu189, His332, Glu333, Asp342, Ala344, and Glu354. The second shell residues Asp61, His337, and Arg357 and the region around the chloride are also included. This region contains, besides chloride, also Lys317 and three water molecules, forming a hydrogen-bonding network, as in the X-ray structure. The core structure of this model is very similar to the old DFT structure.⁵

There is one change of the present model as compared to the one used in the recent studies. In the middle of the present project, it was discovered that the backbone in the His332-Glu333 part of the peptide was not quite optimal. Therefore, reoptimizations of all structures were done, where this part of the backbone more closely followed the high-resolution X-ray structure. The changes had only small effects on the energetics reported previously.

III. RESULTS

Water exchange has been studied in three of the S-states of the OEC and are described below in one subsection each. The

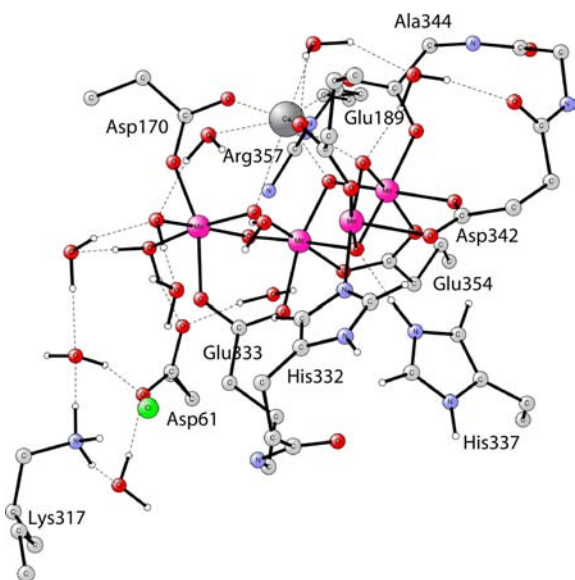


Figure 1. Model used in the present calculations (S_0 -state). The figure is given to show the size of the model and which amino acids are included. For more details, see the Supporting Information.

water exchange in the S_0 -state was left out as being less central than the other ones. For S_4 there is no experimental information. For comparison to the calculated values below, the water exchange rates given in the Introduction are first converted to barriers using transition state theory. For S_1 , the barrier is 20 kcal/mol, for S_2 the barrier is 17 kcal/mol, and for S_3 the two barriers are 17 and 15 kcal/mol, for the slow and fast exchanging water, respectively. The experience is that calculated barriers for this type of processes can be overestimated by a few kcal/mol. It should be added that TS-theory has been shown to work very well for processes higher than 10 kcal/mol.³⁵ This means that detailed dynamical effects, such as those obtained by dynamical modeling, should be insignificant in the present context, at least in relation to the overall accuracy of the present methodology. The present mechanisms were reached after nearly 2 years of calculations. It is difficult to recapitulate the different stages in reaching the final mechanisms, and therefore only the final results will be described here.

One of the most important findings obtained in the present study should first be mentioned. It has been found that a reasonable barrier for an exchange with an outside water only occurs for a water ligand bound to an Mn(III) center of the OEC. This means that for a hydroxo group or an oxo group to be exchanged, it first has to abstract proton(s) from somewhere else to form a bound water molecule. If this water molecule is bound to an Mn(IV) center, this center then has to accept an electron from another center to become an Mn(III) center. It is only at that point a water exchange can occur for the OEC. It should be emphasized that this finding concerns the OEC and is not general for all Mn-complexes. The energy cost for the exchange of a water bound to an Mn(IV) center is composed of two parts. First, the direct exchange is quite high, on the order of 13 kcal/mol. Second, the cost to create an Mn(IV) bound water on the OEC is also quite high. The sum of these costs become prohibitive in all of the S -states studied here. In an earlier study for a much simpler Mn-complex, it was shown that water exchange was possible on an Mn(IV) center.³⁶ The major reason for this is that the energy was set to zero when the water molecule to be exchanged was already in place on the Mn(IV)

center. Also, the complex studied previously was much less rigid than the OEC, allowing relatively large distortions that made the water exchange easier.

a. Water Exchange in S_1 . The starting point for the water exchange in S_1 is the same ground-state structure as in the previous study, with the minor modification mentioned in the computational section. In the structure, all oxo-groups are unprotonated, and one or two substrate oxygens are present.^{10,13,14} In the theoretical water oxidation mechanism discussed previously,^{20,27} only one water was found to be bound in the OEC. Of the manganese atoms, only the outer one, Mn4, see figure, has water derived ligands, one water, and one hydroxo ligand. The oxygen that should be exchanged is an oxo group in the middle of the complex, colored in red in the figures. A schematic mechanism is shown in Figure 2.

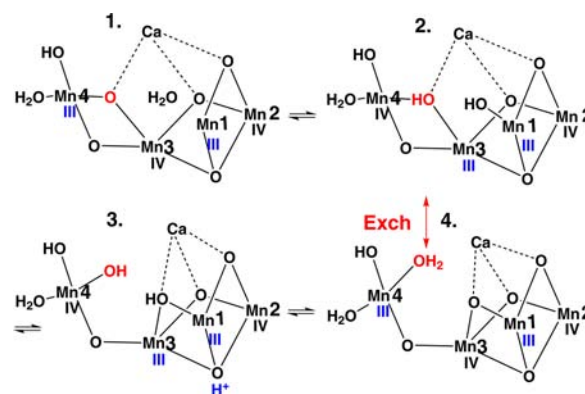


Figure 2. Schematic mechanism for water exchange in the S_1 -state of the OEC. The substrate oxygen is colored in red.

The starting oxidation states are Mn₄(III,IV,IV,III) (1 in the figure). In the first step, an electron is transferred from Mn4 to Mn3 leading to Mn₄(III,IV,III,IV). This is followed by binding of a water molecule to Mn1, where the Jahn–Teller (JT) axis points toward the bound water (2'). The energy is 14.0 kcal/mol higher than for 1. After a subsequent proton transfer from the water to the oxo group, structure 2 is reached with a JT-axis pointing toward Glu189. The energy is now +18.9 kcal/mol. The reason for the high energy of this structure as compared to structure 1 is that the presence of a water ligand on Mn4 leads to a favorable formation of Mn(III), which is not the case for Mn3. This is seen on the sequence of events in water oxidation, where Mn3 is oxidized already in the S_0 to S_1 transition, while Mn4 is oxidized in the S_1 to S_2 transition. The necessary JT-axis change before the next step from structure 2' to 2 also contributes 4.9 kcal/mol to the high energy of 2. An interesting effect occurs in this step involving the protonated His337, which hydrogen bonds to a bridging oxo group. This oxo is positioned along the JT axis of both Mn1 and Mn3, which are both Mn(III) in structure 2. The distance between the oxo group and these Mn-centers should therefore ideally be long, and a very strong hydrogen bond with a distance of only 1.44 Å is therefore formed between the protonated His337 and the oxo, which leads to a natural increase of the Mn–O distances.

The next step is found to be rate-limiting for water exchange in S_1 . At an early stage in this transition, the bridging oxo discussed above becomes protonated from His337 (the proton is colored in blue in Figure 2). After this, the substrate OH (in red) should now leave the connection to Mn3. Instead, the hydroxo group remaining from the outside water should attach

to **Mn3**. This hydroxo group actually becomes bridging between **Mn1** and **Mn3**. The optimized TS is shown in Figure 3, where the proton colored in red is the one donated from

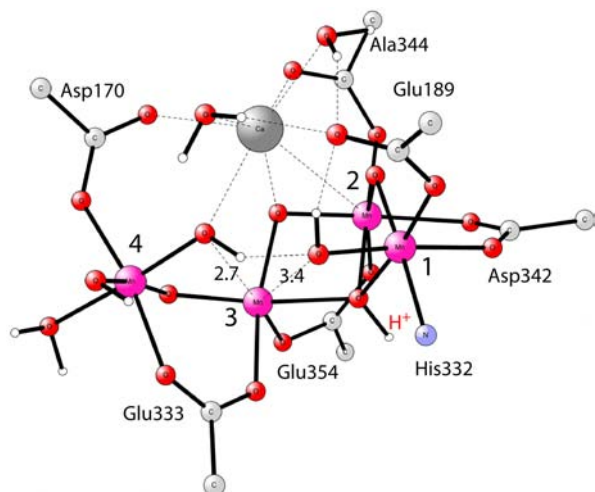


Figure 3. Optimized TS-structure for the rate-limiting step of water exchange in S_1 .

His337 outside the figure. The two key distances are 2.7 Å, between **Mn3** and the protonated oxo, and 3.4 Å between **Mn3** and the other hydroxo. The barrier for this exchange of hydroxo ligands on **Mn3** would be prohibitively high if this center would not be Mn(III), and is the reason for the electron transfer from **Mn4** to **Mn3** in the first step. The calculated barrier counted from **2** is only 2.8 kcal/mol, leading to a total barrier from the starting reactant **1** of 21.7 kcal/mol. The product **3** is still as high as +18.3 kcal/mol, showing the unfavorable situation with **Mn3** as Mn(III) rather than **Mn4** as Mn(III) as in structure **1**.

In the first part of the final step, the substrate hydroxo (in red) becomes fully protonated by taking also the second proton from the other hydroxo group. Because the substrate water is now located on **Mn4**, which is an Mn(IV) center, another electron transfer is needed, this time in the other direction from **Mn3** to **Mn4**. Because it is more favorable to have Mn(III) on **Mn4** than on **Mn3**, the energy goes down from 18.3 to is 11.0 kcal/mol for structure (**4**). Moving the substrate water to a distance 4.0 Å away from **Mn4** is now actually downhill by 3.3 kcal/mol, leading to an energy of +7.7 kcal/mol, where the water exchange takes place. The distance of 4.0 Å was chosen so that the exchanging water should definitely be in the water exchange region. In any case, to move the water even further out costs very little energy. In a previous study, the Mn–O distance for the exchanging water was found to be around 3.0 Å.³⁶ The above steps are then just repeated backward to reach the isotope substituted reactant **1**. The energy diagram is given in Figure 4.

b. Water Exchange in S_2 . The starting structure (**1**) for the S_2 -state exchange is again the same as the ground-state structure from the previous study,²⁷ with the same minor modification as for S_1 . As compared to the S_1 structure, the only change is that **Mn4** has now been oxidized, leading to the oxidation states $Mn_4(III,IV,IV,IV)$. The structure used here was obtained by energy minimization based on an older DFT structure,⁵ modified slightly by the position of Asp170 as found in the recent X-ray structure.⁴ Recently, using a combination of EPR, ENDOR, and DFT, a structure of the S_2 -state was

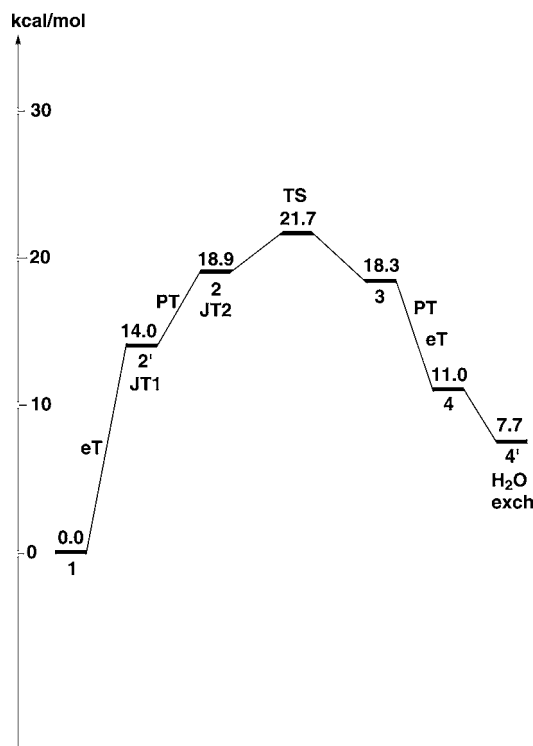


Figure 4. Energy diagram for water exchange in the S_1 -state of the OEC. The numbering of the structures is taken from Figure 2. **JT1** and **JT2** are two different Jahn–Teller distortions of structure **2**, as described in the text.

reached by Ames et al.,³⁷ in almost exact agreement with the one used here. A schematic mechanism for water exchange is shown in Figure 5. For S_2 , already the first step is found to be rate-limiting with a barrier of 17.6 kcal/mol. This is a PCET (proton coupled electron transfer) step, with a concerted electron transfer from **Mn1** to **Mn3** and a proton transfer from the loosely bound water to the substrate oxo group (in red).

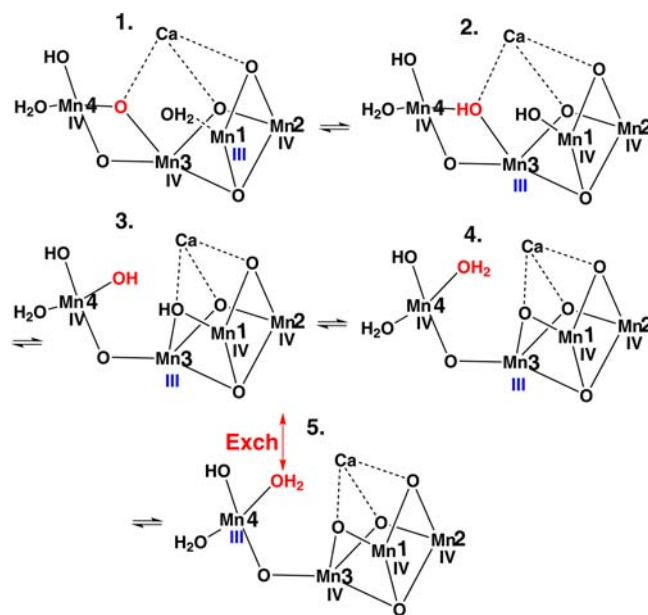


Figure 5. Schematic mechanism for water exchange in the S_2 -state of the OEC. The substrate oxygen is colored in red.

The optimized TS is shown in Figure 6. The proton is almost transferred at the stage when the electron is being transferred,

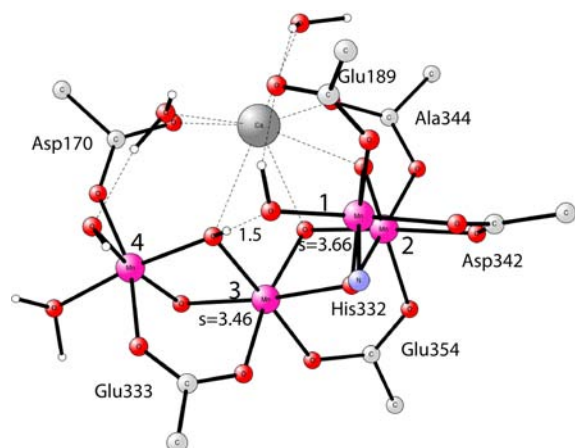


Figure 6. Optimized TS-structure for the rate-limiting PCET step of water exchange in S_2 .

as seen on the rather long O–H distance of 1.5 Å. The electron spin is as usual divided between the two Mn-centers, with spins of 3.46 and 3.66, respectively, as shown in the figure. A typical Mn(III) spin is about 4.0, and for Mn(IV) it is about 3.0. The product (2) energy is at 12.7 kcal/mol, and the oxidation states are $Mn_4(IV,IV,III,IV)$.

After the electron transfer from **Mn1** to **Mn3**, the energy is high at 12.7 kcal/mol, but not as high as in the corresponding electron transfer to **Mn3** in the water exchange in S_1 . The reason is that the accompanying proton transfer in S_2 is favorable. In this way, **Mn1(IV)** in 2 is stabilized in S_2 by a formation of a new Mn–OH bond, and **Mn3(III)** is stabilized by receiving a proton on its ligand. The same advantage does not occur in S_1 . The transfer of the proton to a ligand on **Mn3(III)** is still favorable, but the formation of a new Mn–OH bond on **Mn1(III)** is unfavorable because the oxidation state is not changed.

With the electron transfer made to the critical **Mn3** center, the structure is set up to do the same hydroxide exchange as in the mechanism for S_1 . In contrast to the case of S_1 , there is almost no barrier in S_2 for this step. The energy for the product (3) with the substrate hydroxide moved to **Mn4** is 4.6 kcal/mol. At this stage, there is a proton transfer to the substrate, completing its protonation, from the other hydroxide, which becomes a bridging oxo between **Mn1** and **Mn3**. The energy for the product structure 4 is 8.4 kcal/mol. With the substrate fully protonated and located at center 4, an electron transfer is now made from **Mn3** to **Mn4** to make this center Mn(III), making the water exchange substantially easier. The electron transfer is slightly downhill with 1.5 kcal/mol, leading to an energy of 6.9 kcal/mol for structure 5. The oxidation states are now $Mn_4(IV,IV,IV,III)$. Unlike the situation for S_1 at this stage, moving the substrate water out to a distance of 4.0 Å is an uphill process by 5.2 kcal/mol, leading to an energy of 12.1 kcal/mol, at which point water exchange occurs. The full energy diagram for water exchange in S_2 is shown in Figure 7.

It has recently been suggested that the fast transition between the two S_2 states detected by EPR, with a $g = 2.0$ multiline and a $g = 4.1$ signal, might be important for the mechanism of water exchange.³⁸ In that mechanism, the substrate water would enter at an empty position of **Mn4**,

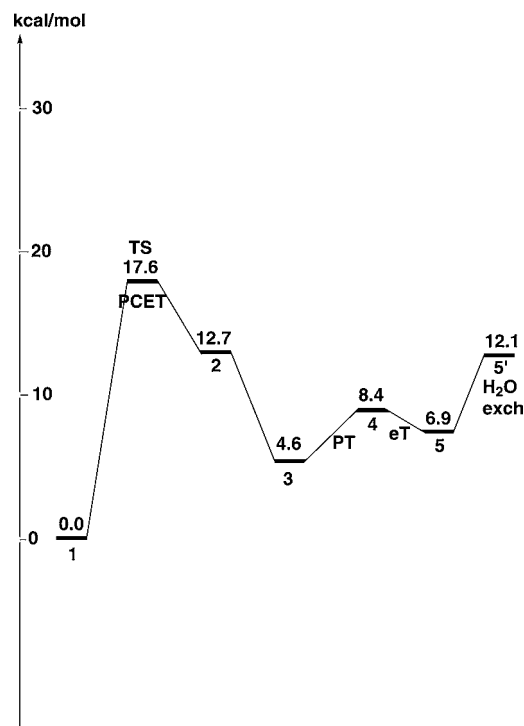


Figure 7. Energy diagram for water exchange in the S_2 -state of the OEC. The numbering of the structures is taken from Figure 5.

rather than at **Mn1** as in the present mechanism. However, that part of the mechanism is the same as the one suggested here, but runs backward starting at 5 in Figure 5, which should be the $g = 4.1$ state. The steps and barriers would thus be exactly the same as here. The key step of the mechanism would still be the one where **Mn3** is reduced, which is needed to do the actual exchange. The other steps, such as the one with the transfer of the oxo-group between **Mn1** and **Mn4**, which should occur in microseconds, would just be part of the general statistical averaging to reach the highest TS.

Ca/Sr substitutions have been found to increase the rate of water exchange in both S_1 and S_2 by about a factor of 4.^{10,17,23} This has been used to suggest direct ligation of the slowly exchanging substrate to both Ca and Mn. While a factor of 4 may seem substantial, it means that the exchange barrier in S_2 would change from the present value of 17.6 kcal/mol to about 17.0 kcal/mol. The effect should of course depend on a difference between Ca and Sr, but must also depend on a differential effect of the interaction in the resting state and in the TS. That effect could be due to a direct effect between Ca/Sr and the oxo ligand, but also on indirect effects by changes of other bond distances. In S_2 the distance between Ca and the exchanging oxo-ligand is 2.68 Å, which changes to 2.57 Å in the TS. The corresponding distances in S_1 are 2.65 and 2.50 Å. Overall, the changes are thus quite small for a Ca–O distance. Furthermore, this Ca–O distance is far from being the one that changes most from the reactant to the TS. From the mechanism given in Figures 2 and 5, it is clear that the Ca–O distance to the incoming water changes by far most, because the nearly free water becomes a bound hydroxide at the TS. There are also a number of other Ca–O distances that change more than the one to the substrate. While the conclusion drawn in the experimental papers appears possible, many other explanations should also be possible. Without a detailed study of the Sr-substituted complex, no conclusion of the origin of

the effect can be drawn on the basis of the present results either, even if the present mechanism and rate-limiting TS for the Ca-case should be correct.

In the present study, it has generally been assumed that a pure electron transfer between two neighboring manganese centers is very fast, because the distance is so short. In some previous studies, it has been shown that fully optimized transition states can be obtained with the conventional techniques also for eT processes. However, in all previous cases, there has been a strong coupling to proton motion, leading to typical adiabatic transitions. This is not the case here in general, and the electron transfers are characterized by a sudden, diabatic transition. The only exception is the PCET step in the S_2 state, for which a fully optimized TS was obtained. Ideally, for the other cases, a method should be used to locate the potential surface crossing points,³⁹ but this will remain for a future project.

c. Water Exchange in S_3 . Before the mechanism for water exchange in S_3 is discussed in detail, one important finding from the previous S-states should be repeated. It was found that a reasonable barrier for an exchange with an outside water only occurs if there is an Mn(III) center somewhere. This means that there is a problem for water exchange in S_3 because there is no Mn(III) center. If not an entirely different mechanism is found, an electron donor outside of the OEC has to be introduced. So far, the attempts to find a different mechanism involving only Mn(IV) were unsuccessful.

The only reasonable electron donor in the proximity of the OEC is the tyrosine Tyr_Z. Experimental findings in this context are very important.^{40–42} For example, Geijer et al. found an EPR signal induced by a change to alkaline pH in the S_3 state. The signal was interpreted as due to a spin-coupled S_2 Tyr_Z state. In the oxygen evolving PSII, the Tyr_Z state in the S_2 to S_3 transition is stable only for a millisecond, but the new state was found to be stable for 5–6 min. It was also found to be more stable than the corresponding state found earlier in Ca-depleted samples, which is stable for 5–15 s. The conclusion drawn was that the new state has an S_2 component that is proton depleted as compared to the normal one observed in water oxidation. In summary, these observations mean that there is a Tyr_Z state that has an energy at normal pH, which is only about 2 kcal/mol higher than the S_3 state. This in turn means that it is possible with very little energy from S_3 to reach a state that has an Mn(III) center. This should therefore in principle allow a mechanism for water exchange in S_3 similar to the one for S_2 discussed above. In support for this conclusion, the experimental result for the slow water exchange in S_3 gave a rate similar to that in S_2 . The only difference is that the S_2 state may not be exactly the same in the two cases.

In the previous study, the S_2^0 state, which should correspond to the normal stable S_2 state observed experimentally in water oxidation, is as much as 11.4 kcal/mol higher in energy than the S_3 state; see Figure 19 in ref 27. The next state after the stable S_2 state considered in the previous study is when P_{680}^+ is created in the S_2 to S_3 transition. This was suggested to lead to a proton expulsion from the OEC and thus to a creation of an $S_2^{-1}P_{680}^+$ state with one proton less than the S_2^0 state. This S_2^{-1} state, without a tyrosyl radical but with P_{680}^+ , is still 8.0 kcal/mol less stable than the S_3 state. Two conclusions can be drawn from this difference from the experiments that show an S_2 state only 2 kcal/mol higher than the S_3 state. The first one is that the experimentally observed S_2 Tyr_Z state should be more stable than the $S_2^{-1}P_{680}^+$ state, but probably not by more than 4 kcal/

mol. This still leaves a discrepancy to experiments of 2 kcal/mol, and a second conclusion is therefore that there is a minor error in the methods or models used in the calculations. This can still not be regarded as a major problem considering the normal inaccuracy of DFT. A more physical origin of the problem could be the treatment of entropy effects. Except for the release of O₂ and the binding of water from the bulk to the model, entropy effects were assumed to be small. One step where this assumption could be problematic is in the S_2 to S_3 transition, where a very weakly bound water molecule becomes bound as a hydroxide with a short Mn–O bond. An attempt was therefore made to estimate the entropy effect in this step. To do this, a smaller model was required where no atoms are fixed during the geometry optimization. Hessians were therefore computed for the same model as used here for the zero-point effects, but with a release of all constraints. The result found was indeed a loss of entropy in this transition, calculated to be 2.6 kcal/mol. It should be added that the rate of the transition between S_3 and S_2 Tyr_Z is unimportant for the water exchange rate as long as it is not slower than 2 and 40 s⁻¹, for the slow and fast exchange, respectively, which can safely be excluded.

Another conclusion drawn from the above considerations is that the S_2 Tyr_Z state observed in the experiments most likely has an S_2^{-1} component, which has one proton less than the normal S_2^0 state. This conclusion is very similar to, if not the same as, the one drawn in one experimental study.⁴¹ The proton missing is according to the present calculations, one on the water ligand on Mn4.

The only question remaining is whether there is any significant difference as compared to water exchange in S_2 from the missing proton. This is not expected because the missing proton is on a ligand on Mn4, which is not involved in the rate-limiting step; see above for S_2 . Still calculations were done without the proton, and a barrier just slightly lower than the one in S_2 was obtained, 16.4 kcal/mol counted from S_2^{-1} as compared to 17.6 kcal/mol for S_2^0 . Because the measured rates for water exchange are the same for S_2 and S_3 , but there is an energy cost to reach the Mn(III) reactant for S_3 , the barrier should actually be slightly lower, but this agreement with experiments must be regarded as fortuitous. In summary, the slow water exchange in S_3 has almost exactly the same mechanism as the one in S_2 , with a similar rate, in agreement with experiments.¹⁸

The conclusion that had to be drawn above that the S_2 Tyr_Z state is more stable than the $S_2^{-1}P_{680}^+$ state was initially rather surprising. This means that about 4 kcal/mol seems to be wasted in the electron transfer between Tyr_Z and P_{680}^+ , which leads to a nearly 1000-fold decrease of the rate of the next step leading to the final S_3 state in water oxidation. This sacrifice in rate is probably made to make the charge separation more stable. The new conclusion also leads to a slightly different scenario for the beginning of the S_2 to S_3 transition. Rather than the $S_2^{-1}P_{680}^+$ intermediate, which was the one discussed in the previous paper,²⁷ there should be an S_2^{-1} Tyr_Z intermediate that is more stable by 4 kcal/mol than the previous one.

The fast water exchange in S_3 finally should be just the reverse of the water oxidation step from S_2^{-1} to S_3^0 . In the previous study, this step gave a reverse barrier of 17.0 kcal/mol. This is somewhat higher than the experimentally determined water exchange barrier of 15 kcal/mol. Again, this could be due to the neglect of entropy in this step in the previous calculations.

d. Water Exchange on Calcium. As mentioned in the Introduction, a completely different mechanism has been suggested for water oxidation by Sproviero et al.¹⁶ and by Pecoraro et al.⁴³ In that mechanism, the slowly exchanging water should be bound to calcium. Using a DFT model, a quite high barrier of 17–19 kcal/mol for water exchange was indeed found. The high barriers were found to be due to incomplete solvation shells. In the present study, it was instead found that there are a large number of water molecules outside calcium, which are bound better than in bulk water and therefore present in this region. A transition state was obtained for the S_2 state, following the general procedure described in section II, with a barrier of only 8.6 kcal/mol, not counting entropy effects that should lower the barrier further. The distances from calcium to the two exchanging waters are 3.44 and 4.05 Å, respectively. This result is in line with the very fast exchange rates observed for calcium complexes in solution of 10^8 s^{-1} ,²² but it excludes a water on calcium as being the slowly exchanging water observed, which exchanges very much slower, on the order of seconds.

IV. CONCLUSIONS

A complete mechanism for water oxidation at the OEC of PSII, based on DFT calculations, has been described in a series of papers the past decade; see, for example, refs 5,20,25,27. A leading principle has been to always select the structure with the lowest energy.⁴⁴ In this way, arbitrariness has been avoided, and a steady progress has been guaranteed. The water oxidation mechanism obtained is consistent with a vast, and growing, amount of experimental information. One of the most surprising features of the mechanism is that it requires that one substrate oxygen is bound as a bridging oxo group in the center of the OEC. This becomes even more surprising in light of the water exchange experiments that show that this oxygen can be exchanged with oxygen from solvent water faster than seconds both in the S_2 and in the S_3 state. This is a very unusual feature for a metal bridging oxo-group and has therefore been the feature of the mechanism hardest to accept.^{15,16,19}

In the present study, water exchange has been studied in the S_1 , S_2 , and S_3 states using the same type of methods and models that were previously used to deduce the water oxidation mechanism. One important result found is that water exchange at a reasonable rate for the OEC only occurs with a water molecule bound to an Mn(III) center. A key to the exchange is furthermore that **Mn3** has to be reduced to an Mn(III) state to release the bond to the substrate oxygen. This means that the mechanism has to contain several steps, leading to a much more complicated water exchange mechanism than previously assumed.^{14–17} This also explains why it has been so difficult to obtain a conclusive mechanism for water oxidation based on these experiments. It is also directly seen from the present mechanism why water exchange results for model dimers are not representative for the OEC.¹⁹ For example, in the rate-limiting step for S_1 (see Figure 3), two manganese are needed to hold the hydroxides, while the Mn–O bond exchange occurs on a third manganese. A similar situation occurs also for S_2 . Recent more refined experiments for the OEC have changed the situation,²⁴ and more definitive conclusions have been possible to draw.

In summary, water exchange in S_1 is limited by a hydroxide exchange on the **Mn3** center in a Mn(III) oxidation state. The high barrier of 21.7 kcal/mol (exp. 20 kcal/mol) is due to both an unfavorable electron transfer from **Mn4** to **Mn3**, and a

costly change of JT-axis required for the hydroxide exchange. Water exchange in S_2 goes through a similar mechanism, but here the electron transfer from **Mn1** to create a Mn(III) state for **Mn3** occurs via a PCET process, which has a lower rate-limiting barrier of 17.6 kcal/mol (exp. 17 kcal/mol). The PCET barrier in S_2 is lower because a new Mn–OH bond can be formed on **Mn1**, which obtains oxidation state IV in this process. In S_1 the same advantage is not possible, because **Mn1** has oxidation state III. The slow water exchange in S_3 is suggested to occur by the same mechanism as in S_2 (exp. barrier 17 kcal/mol). This is possible because there is an $S_2\text{Tyr}_2^-$ state with only a slightly higher energy than S_3 . The transition between these states does not slow water exchange as long as the transition is faster than the water exchange, which can safely be assumed. The slow water exchange then occurs for an S_2^{-1} state with one less proton as compared to the normal S_2 state. The missing proton is suggested to come from the water molecule on **Mn4**. Without this proton, water exchange is actually slightly faster than in S_2 . The fast water exchange in S_3 occurs by the reverse of the S_2^{-1} to S_3 transition with a barrier of 17.0 kcal/mol (exp. 15 kcal/mol).

It should finally be stated that in theoretical studies of the present type, it is not possible to be certain that the correct mechanism has been found. However, it can safely be concluded that other mechanisms tried with much higher barriers cannot be right. Furthermore, a viable alternative to the present mechanism has to have almost the same rate as those found here. A new mechanism found that is either much slower or much faster therefore has to be wrong. In the latter case, it would indicate an error in either the model or the method used.

■ ASSOCIATED CONTENT

■ Supporting Information

Coordinates for structures in the figures and diagrams. This material is available free of charge via the Internet at <http://pubs.acs.org>.

■ AUTHOR INFORMATION

Corresponding Author

ps@physto.se

Notes

The authors declare no competing financial interest.

■ REFERENCES

- (1) Ferreira, K. N.; Iverson, T. M.; Maghlaoui, K.; Barber, J.; Iwata, S. *Science* **2004**, *303*, 1831–1838.
- (2) Loll, B.; Kern, J.; Saenger, W.; Zouni, A.; Biesiadka, J. *Nature* **2005**, *438*, 1040–1044.
- (3) Guskov, A.; Kern, J.; Gabdulkhakov, A.; Broser, M.; Zouni, A.; Saenger, W. *J. Nat. Struct. Biol.* **2009**, *16*, 334–341.
- (4) Umena, Y.; Kawakami, K.; Shen, J.-R.; Kamiya, N. *Nature* **2011**, *473*, 55–60.
- (5) Siegbahn, P. E. M. *Chem.-Eur. J.* **2008**, *27*, 8290–8302.
- (6) Yano, J.; Kern, J.; Sauer, K.; Latimer, M. J.; Pushkar, Y.; Biesiadka, J.; Loll, B.; Saenger, W.; Messinger, J.; Zouni, A.; Yachandra, V. K. *Science* **2006**, *314*, 821–825.
- (7) Haumann, M.; Muller, C.; Liebisch, P.; Iuzzolino, L.; Dittmer, J.; Grabolle, M.; Neisius, T.; Meyer-Klaucke, W.; Dau, H. *Biochemistry* **2005**, *44*, 1894–1908.
- (8) Yano, J.; Kern, J.; Irrgang, K.-D.; Latimer, M. J.; Bergmann, U.; Glatzel, P.; Pushkar, Y.; Biesiadka, J.; Loll, B.; Sauer, K.; Messinger, J.; Zouni, A.; Yachandra, V. K. *Proc. Natl. Acad. Sci. U.S.A.* **2005**, *102*, 12047–12052.

- (9) Messinger, J.; Badger, M.; Wydrzynski, T. *Proc. Natl. Acad. Sci. U.S.A.* **1995**, *92*, 3209–3213.
- (10) Hillier, W.; Messinger, J.; Wydrzynski, T. *Biochemistry* **1998**, *37*, 306–317. Hillier, W.; Wydrzynski, T. *Biochim. Biophys. Acta* **2001**, *1503*, 197–209. Hillier, W.; Wydrzynski, T. *Phys. Chem. Chem. Phys.* **2004**, *6*, 4882–4889. Hillier, W.; Wydrzynski, T. *Coord. Chem. Rev.* **2008**, *252*, 306–317. Hendry, G.; Wydrzynski, T. *Biochemistry* **2003**, *42*, 6209–6217.
- (11) Singh, S.; Debus, R. J.; Debus, T.; Wydrzynski, T.; Hillier, W. *Philos. Trans. R. Soc.* **2003**, *363*, 1229–1234.
- (12) Hendry, G.; Wydrzynski, T. *Biochemistry* **2008**, *41*, 13328–13334.
- (13) Noguchi, T. *Philos. Trans. R. Soc. London, Ser. B* **2008**, *363*, 1189–1195.
- (14) Messinger, J.; Renger, G. In *Primary Processes of Photosynthesis: Principles and Apparatus, Comprehensive Series in Photochemical and Photobiological Sciences*; Renger, G., Ed.; RSC Publishing: Cambridge, UK, 2008; Vol. 9, pp 291–349.
- (15) Dau, H.; Limberg, C.; Reier, T.; Risch, M.; Roggan, S.; Strasser, P. *ChemCatChem* **2010**, *2*, 724–761.
- (16) Sproviero, E. M.; Shinopoulos, K.; Gascon, J. A.; McEvoy, J. P.; Brudvig, G. W.; Batista, V. S. *Philos. Trans. R. Soc. London, Ser. B* **2008**, *363*, 1149–1156.
- (17) Cox, N.; Messinger, J. *Biochim. Biophys. Acta* **2013**, <http://dx.doi.org/10.1016/j.bbabi.2013.01.013>.
- (18) Messinger, J.; Noguchi, T.; Yano, J. In *Molecular Solar Fuels*; Wydrzynski, T., Hillier, W., Eds.; RSC Publishing: Cambridge, UK, 2011.
- (19) McConnell, I. L.; Grigoryants, V. M.; Scholes, C. P.; Myers, W. K.; Chen, P.-Y.; Whittaker, J. W.; Brudvig, G. W. *J. Am. Chem. Soc.* **2012**, *134*, 1504–1512.
- (20) Siegbahn, P. E. M. *Chem.-Eur. J.* **2006**, *12*, 9217–9227.
- (21) Siegbahn, P. E. M.; Crabtree, R. H. *J. Am. Chem. Soc.* **1999**, *121*, 117–127.
- (22) Helm, L.; Merbach, A. E. *Chem. Rev.* **2005**, *105*, 1923–1959.
- (23) Messinger, J. *Phys. Chem. Chem. Phys.* **2004**, *6*, 4764–4771.
- (24) Rapatskiy, L.; Cox, N.; Savitsky, A.; Ames, W. M.; Sander, J.; Nowaczyk, M. M.; Rögner, M.; Boussac, A.; Neese, F.; Messinger, J.; Lubitz, W. *J. Am. Chem. Soc.* **2012**, *134*, 16619–16634.
- (25) Siegbahn, P. E. M. *Acc. Chem. Res.* **2009**, *42*, 1871–1880.
- (26) Siegbahn, P. E. M. *ChemPhysChem* **2011**, *12*, 3274–3280.
- (27) Siegbahn, P. E. M. *Biochim. Biophys. Acta* **2012**, <http://dx.doi.org/10.1016/j.bbabi.2012.10.006>.
- (28) Becke, A. D. *J. Chem. Phys.* **1993**, *98*, 5648–5652.
- (29) Reiher, M.; Salomon, O.; Hess, B. A. *Theor. Chem. Acc.* **2001**, *107*, 48–55.
- (30) Grimme, S. *J. Chem. Phys.* **2006**, *124*, 034108. Schwabe, T.; Grimme, S. *Phys. Chem. Chem. Phys.* **2007**, *9*, 3397–3406.
- (31) Siegbahn, P. E. M. *J. Biol. Inorg. Chem.* **2006**, *11*, 695–701.
- (32) *Jaguar 5.5*; Schrödinger, LLC: Portland, OR, 1991–2003.
- (33) Frisch, M. J.; Trucks, G. W.; Schlegel, H. B.; Scuseria, G. E.; Robb, M. A.; Cheeseman, J. R.; Scalmani, G.; Barone, V.; Mennucci, B.; Petersson, G. A.; Nakatsuji, H.; Caricato, M.; Li, X.; Hratchian, H. P.; Izmaylov, A. F.; Bloino, J.; Zheng, G.; Sonnenberg, J. L.; Hada, M.; Ehara, M.; Toyota, K.; Fukuda, R.; Hasegawa, J.; Ishida, M.; Nakajima, T.; Honda, Y.; Kitao, O.; Nakai, H.; Vreven, T.; Montgomery, J. A., Jr.; Peralta, J. E.; Ogliaro, F.; Bearpark, M.; Heyd, J. J.; Brothers, E.; Kudin, K. N.; Staroverov, V. N.; Kobayashi, R.; Normand, J.; Raghavachari, K.; Rendell, A.; Burant, J. C.; Iyengar, S. S.; Tomasi, J.; Cossi, M.; Rega, N.; Millam, N. J.; Klene, M.; Knox, J. E.; Cross, J. B.; Bakken, V.; Adamo, C.; Jaramillo, J.; Gomperts, R.; Stratmann, R. E.; Yazyev, O.; Austin, A. J.; Cammi, R.; Pomelli, C.; Ochterski, J. W.; Martin, R. L.; Morokuma, K.; Zakrzewski, V. G.; Voth, G. A.; Salvador, P.; Dannenberg, J. J.; Dapprich, S.; Daniels, A. D.; Farkas, Á. ě.; Foresman, J. B.; Ortiz, J. V.; Cioslowski, J.; Fox, D. J. *Gaussian 09*, revision A.1; Gaussian, Inc.: Wallingford, CT, 2009.
- (34) Siegbahn, P. E. M. *Phys. Chem. Chem. Phys.* **2012**, *14*, 4849–4856.
- (35) Olsson, M. H. M.; Mavri, J.; Warshel, A. *Philos. Trans. R. Soc. London, Ser. B* **2006**, *361*, 1417–1432. Pislakov, A. V.; Cao, J.; Kamerlin, S. C. L.; Warshel, A. *Proc. Natl. Acad. Sci. U.S.A.* **2009**, *106*, 17359–17364.
- (36) Lundberg, M.; Blomberg, M. R. A.; Siegbahn, P. E. M. *Theor. Chem. Acc.* **2003**, *110*, 130–143.
- (37) Ames, W.; Pantazis, D. A.; Krewald, V.; Cox, N.; Messinger, J.; Lubitz, W.; Neese, F. *J. Am. Chem. Soc.* **2011**, *133*, 19743–19757.
- (38) Pantazis, D. A.; Ames, W.; Cox, N.; Lubitz, W.; Neese, F. *Angew. Chem., Int. Ed.* **2012**, *51*, 1–7.
- (39) Harvey, J. N.; Aschi, M.; Schwarz, H.; Koch, W. *Theor. Chem. Acc.* **1998**, *99*, 95.
- (40) Vos, M. H.; Gorkom, H. J.; van Leeuwen, P. J. *Biochim. Biophys. Acta* **1991**, *1056*, 27. de Wijn, R.; van Gorkum, H. J. *Photosynth. Res.* **2002**, *72*, 217–222.
- (41) Geijer, P.; Morvaridi, F.; Styring, S. *Biochemistry* **2001**, *40*, 10881–10891.
- (42) Rappaport, F.; Diner, B. A. *Coord. Chem. Rev.* **2008**, *252*, 259–272.
- (43) Pecoraro, V. L.; Baldwin, M. J.; Caudle, M. T.; Hsieh, W. Y.; Law, N. A. *Pure Appl. Chem.* **1998**, *70*, 925–929.
- (44) Siegbahn, P. E. M. *J. Am. Chem. Soc.* **2009**, *131*, 18238–18239.